Supporting information for

Probing the Selectivity of a Nanostructured Surface by Xenon Adsorption

Roland Widmer*[a], Daniele Passerone[b], Thomas Mattle[a,c], Hermann Sachdev[d] and Oliver Gröning[a]

Simulation details

We used for our simulations the package cp2k (http://cp2k.berlios.org), with the classical mechanics module FIST. We kept the coordinates of the substrate (1 ML BN + 3 layers of Rhodium) fixed at the values obtained by Laskowski [1] with his DFT simulations. We considered a unit cell with 16 nanomesh pores, with periodic boundary conditions in the planar directions parallel to the surface. The temperatures were tuned using a Nose thermostat, and the interaction potentials of Xe with itself and other species were all pairwise.

In particular, we used Lennard-Jones potentials for the interaction with B and N atoms, using as starting point the parameters suggested by Migone et al. [2], that is $\varepsilon_{Xe\text{-}B}= \varepsilon_{Xe\text{-}N}$ =0.00673 eV and $\sigma_{Xe\text{-}B}= \sigma_{Xe\text{-}N}$ =3.72 Å. We call this potential V{S1}. Concerning the interaction with rhodium, we used data for C_3 parameters for Rh and other metals [3] for fitting the ε and σ coefficients accordingly. Eventually, we found $\varepsilon_{Xe\text{-}Rh}$ =0.017 eV and $\sigma_{Xe\text{-}Rh}$=3.28 Å.

Concerning Xe-Xe interactions, we adopted the most faithful potential that is able to reproduce the correct structure of Xe in the solid state, namely the HFD-B potential by Aziz and Slaman [4]. Although of different form, particularly in the repulsive part, this potential has a similar shape as a Lennard-Jones potential with ε =0.00243 eV and σ=3.89 Å.

Since we are neglegting several effects (dipolar forces, charge transfer, collective interactions) we used the available experimental data (orientation of the Xe overlayer, selectivity of the pores) to tune the Xe-BN interaction potential. We found that only by doubling the strength $\varepsilon_{Xe\text{-}B}= \varepsilon_{Xe\text{-}N}$ we could reproduce most of the experimental observations; whereas the potential V{S1} lead instead to no selectivity of the pores (see **Fig. S1**). Thus, the potential V{S2}, with $\varepsilon_{Xe\text{-}B}= \varepsilon_{Xe\text{-}N}$ =0.0134 eV

was used throughout. As we will see and describe in the manuscript the doubling of the pair potential implicitly takes into account the electrostatic component of the Xe-nanomesh interaction.

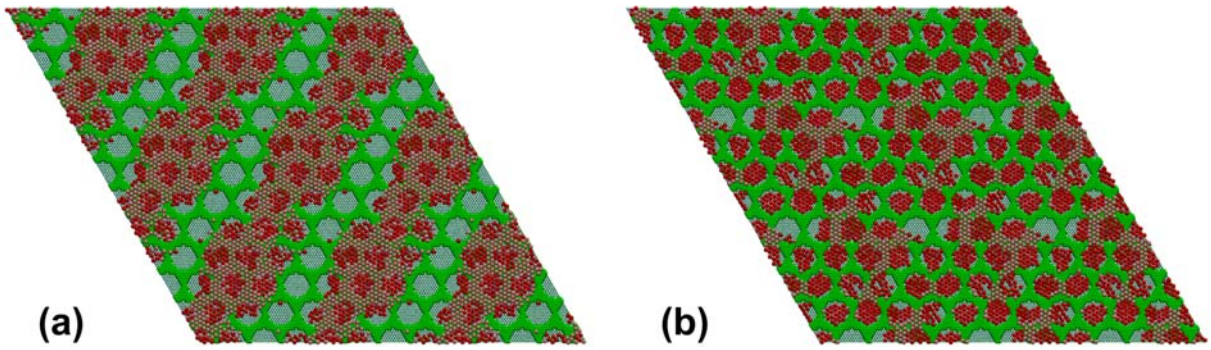

Figure S1: (a) final configuration starting from all Xe in the wires, with the substrate potential V{S1}. Only substrate atoms in the wires (in green) are shown. Pink Xe atoms in the wires connect several islands; the orientation of these islands is compatible with experiments. (b) The connectivity is much reduced with the potential V{S2}. In both cases the pores present correctly oriented islands, but only in the second case there is selectivity between pores and wires. 4 simulations cells (64 pores) are shown.

We also addressed the issue of ring stability and we played with the relative strength of the Xe-Xe and Xe-BN potentials. We found that, upon decreasing the Xe-Xe interactions, 12-membered rings became more stable with respect to 12-membered islands located in the center of the pore.

In **Fig. S2**, the number of atoms in pores and wires were plotted as a function of the coverage after annealing, subsequent cooling and minimization. The number of atoms per pore in the filled pores (with more than 8 Xe atoms) remains above 20 for all coverages larger than 0.4, and for coverages smaller than 0.5 the number of atoms in the wires substantially decreases

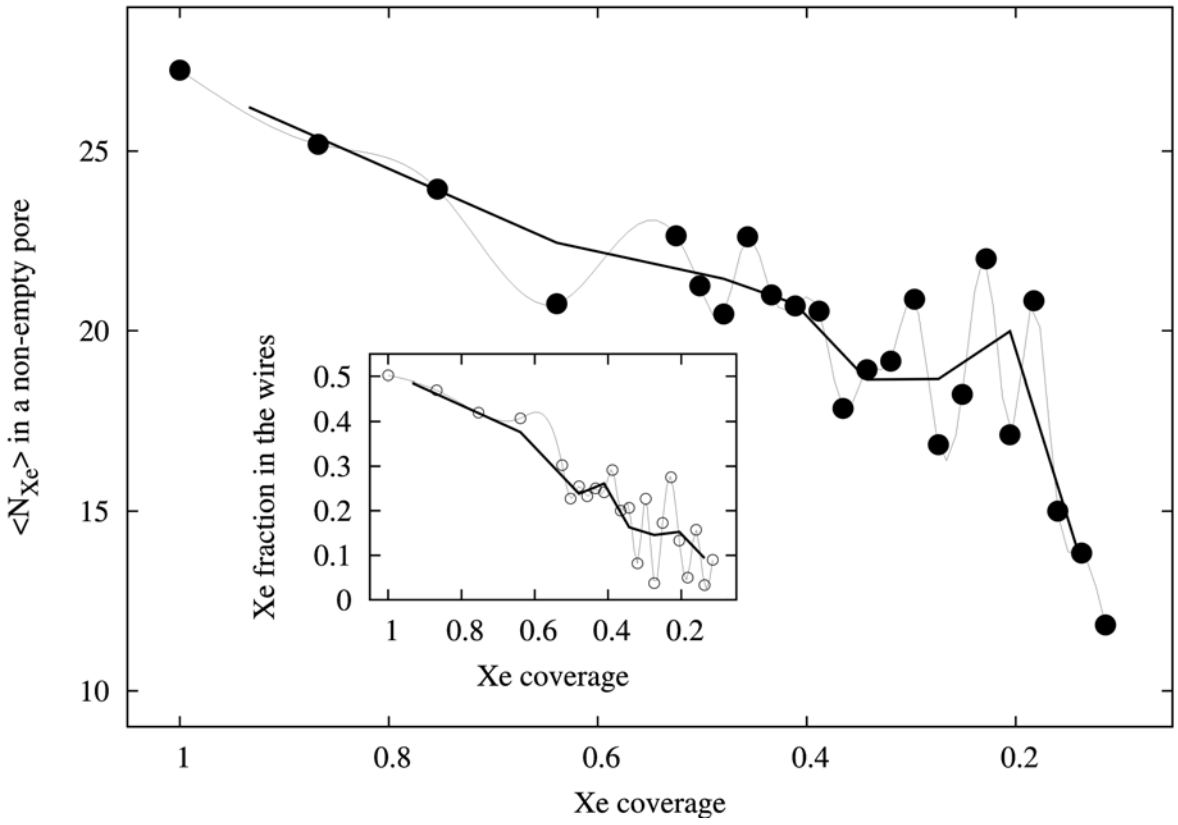

Figure S2: Average number of atoms in a non-empty pore and fraction of Xe in the wires (inset) as a function of Xe coverage. The bold line represents a running average with 3 points, whereas the dashed line just serves as guide to the eye.

The existence of Xe rings was explained in [5] in terms of the interaction of the electric field, arising from surface potential difference between pores and wires of the nanomesh, with polarizable Xe atoms. This leads to preferred adsorption sites in the zones of highest magnitude of the electric field, i.e. at the pore border. We performed independent continuum finite element calculations, which indeed support that this is the case.

These simulations are preformed in cylindrical coordinates (r,z) with the origin in the centre of the nanomesh pore. At z=0 nm, the van der Waals surface so to speak, we consider three regions with fixed potentials $r_1=\{0,r_p\}$ at ϕ_1, $r_2=\{ r_p,r_w\}$ at ϕ_2 and $r_3>r_w$ at ϕ_3. Region r_1 represents the pore, region r_2 the wire and region r_3 the average potential of pores and wires at some distance from the central

pore. For this configuration we solve numerically the Laplace equation for the sufficiently large vacuum region z={0, 6.0 nm} and r={0, 6.0 nm} with natural boundary conditions.

First, we discuss the case, where we have reproduced the potential as obtained from the DFT calculations published in [5], which we call the Blaha potential. The used parameters are:

r_p=0.61 nm, r_w=2.37 nm, ϕ_1=-831 meV, ϕ_2=+0.039 meV and ϕ_3-191 meV.

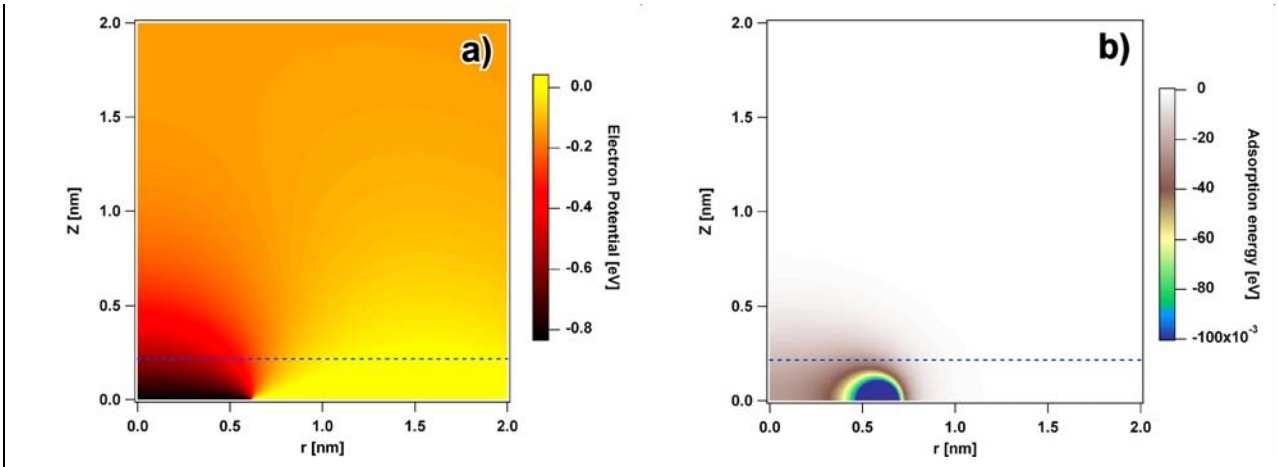

Figure S3: a) Map of the electron potential above a pore for the Blaha potential parameters. b) Map of the Xe polarization adsorption potential according to $A_{Xe}(r,z)=-1/2*E(r,z)^2*\alpha$, where E(r,z) is the magnitude of the electric field and a the polarizability of a Xe atom. The blue dotted line represents the adsorption height of Xe equal to the van der Waals radius 0.216 nm.

Figure S3 shows the results of the simulations for the parameter set given above, one can see that there are considerable lateral and vertical potential gradients present. **Figure S4** reports the electron potential and the Xe adsorption potential at the adsorption height of z=0.216 nm for two simulations. The blue curves in Fig. S4 correspond to the case where we assume a surface potential difference of 560 meV and the red curves the situation for a difference on 320 meV as referred from experiment. As can be seen in the upper graph, the simulated potential for the 560 meV case fits very well the shape of the DFT calculated Blaha potential, which is represented here by an analytical curve fitted to the data of [5]. The corresponding curves of the Xe adsorption are shown in the lower graph.

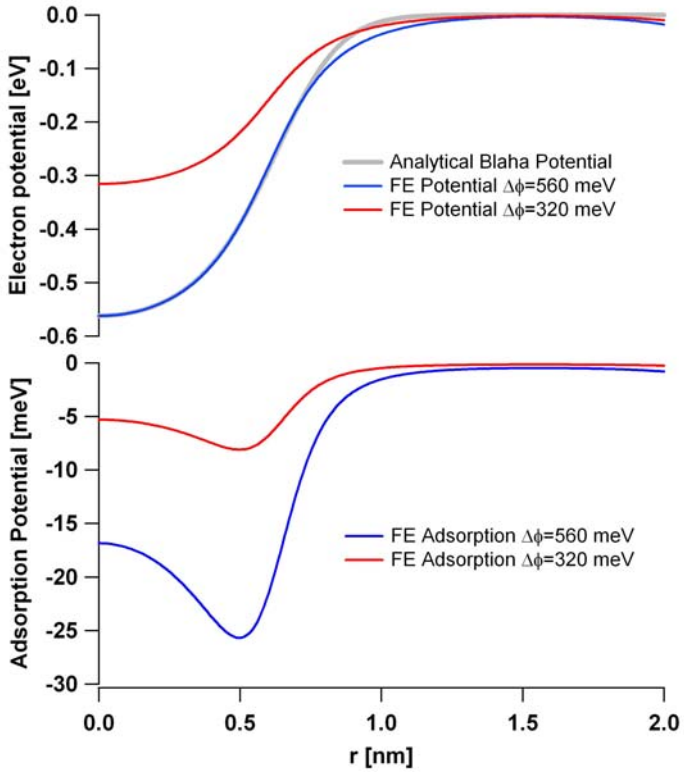

Figure S4: Upper graph: Electrostatic potential curves at z=0.216 nm for the Blaha potential (light gray) and two cases of different surface potential differences between pores and wires. Low graph: Xe adsorption potential at z=0.216 nm for the two cases.

One can observe clearly that the minimum of the adsorption potential is located around r=0.5 nm and therefore the pore rim. For the $\Delta\phi$=560 meV case the adsorption potential difference between rim and wire is 25.2 meV, the difference between rim and pore center is however only 8.8 meV. This is due to the fact that with such a small pore diameter and large surface potential difference string vertical electric fields occur, responsible for a strong adsorption also at the pore center. In comparison to the $\Delta\phi$=320 meV case, one can see how sensitive the magnitude of the adsorption potential is on the surface potential difference.

With regard to our experimental observation the Blaha potential yields a rim radius which is significantly too small. Therefore we have used a second set of parameters, which reproduces the

same surface potential difference as in the case above but with a rim radius of 1.0 nm. The results of the simulation are shown in **Fig. S5**.

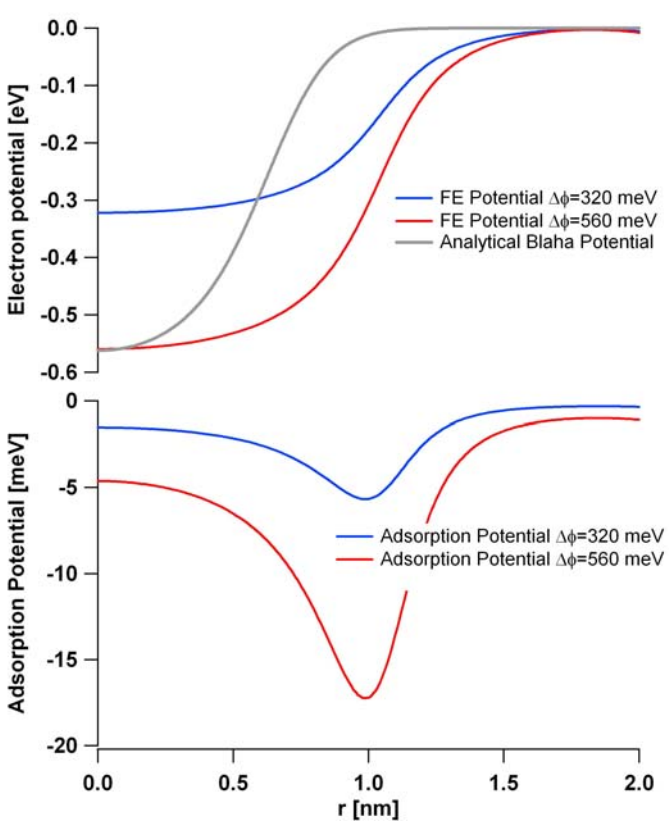

Figure S5: Upper graph: Electrostatic potential curves at z=0.216 nm for the Blaha potential (light gray) and two cases of different surface potential differences between pores and wires, with r_p=1.05 nm. Low graph: Xe adsorption potential at z=0.216 nm for the two cases.

Due to the large pore size the contribution of vertical field components is not as strong as in the r_p=0.61 nm case, this reduces the magnitude of the adsorption potential in the center of the pore. The adsorption energy difference between rim and wire is now 16.2 meV and between rim and center of the pore 12.6 meV. The lower vertical field components also reduce the difference between rim and wire. When we look at the Δϕ=320 meV case the magnitude of the adsorption potential is again strongly reduced. The adsorption energy difference between rim and pore is in

this later case only 5.3 meV, which scales correctly with square of the surface potential differences 16.2 meV*(320/560)^0.5=5.29 meV.

It should be noted here that the assumption of an abrupt surface potential change at z=0 nm and $r=r_p$ over estimates the electric field as the surface potential change should be smoothed out by screening of the Rh valence electrons. In this sense the $\Delta\phi$=560 meV we discuss here represents an upper limit of the electrostatic contribution to the Xe polarization induced adsorption potential.

References

[1] R. Laskowski, P. Blaha, *J. Phys. Cond. Mat.* 2008, **20**, 064207

[2] A.D. Migone, M.T. Alkhafaji, C. Vidali, M. Karimi, *Phys. Rev. B* 1993, **47**, 6685

[3] C. Schwartz, R. J. Le Roy, *Surf. Sci.* 1986, **166**, L141

[4] R. A. Aziz, M. J. Slaman, *Mol. Phys.* 1986, **57**, 825

[5] H. Dil, J. Lobo-Checa, R. Laskowski, P. Blaha, S. Berner, J. Osterwalder, T. Greber, *Science* 2008, **319**, 1824